

# Fabrication of micronozzles using low-temperature wafer-level bonding with SU-8

Sheng Li<sup>1</sup>, Carl B Freidhoff<sup>2</sup>, Robert M Young<sup>2</sup>  
and Reza Ghodssi<sup>1</sup>

<sup>1</sup> MEMS Sensors and Actuators Lab, Department of Electrical and Computer Engineering,  
The Institute for Systems Research, University of Maryland, College Park, MD 20742, USA

<sup>2</sup> Northrop Grumman Electronic Systems Inc., Baltimore, MD 21203, USA

Received 19 February 2003, in final form 23 April 2003

Published 20 June 2003

Online at [stacks.iop.org/JMM/13/732](http://stacks.iop.org/JMM/13/732)

## Abstract

This paper describes a method for fabricating micronozzles using low-temperature wafer-level adhesive bonding with SU-8. The influence of different parameters on the bonding of structured wafers has been investigated. The surface energies of bonded wafers are measured to be in the range of 0.42–0.56 J m<sup>-2</sup>, which are comparable to those of some directly bonded wafers. Converging–diverging nozzle structures with throat widths as small as 3.6 μm are formed in an SU-8 film bonded with another SU-8 intermediate layer to produce sealed micronozzles. A novel interconnection technique is developed to interface and test the micronozzles with a macroscopic fluid delivery system to demonstrate the feasibility of the fabrication process. Leakage test results show that this low-temperature wafer bonding process is a viable MEMS fabrication technique for microfluidic applications.

(Some figures in this article are in colour only in the electronic version)

## 1. Introduction

Microfluidic devices are becoming prevalent, both in commercial applications and scientific investigations. There has been recent, rapid development of MEMS-based fluidic devices working in gaseous environments under standard atmospheric conditions [1]. Gas flow in microchannels has become the subject of intensive research because of its wide variety of applications such as gas sensors, micro cooling devices, etc. It is also fundamental to the understanding of microscale fluid mechanics [2, 3]. Conventional flow models, such as the Navier–Stokes equations, with a no-slip boundary condition at the fluid–solid interface, have been routinely and successfully applied to traditional fluid devices. Fluid flows in micro devices, however, differ from those in macroscopic ones. The performance of MEMS-based ducts, nozzles, valves, turbo-machines, etc, cannot always be correctly predicted or described using these models. Many questions have been raised when measurements carried out in micro devices could not be explained via traditional flow modeling. For example, the pressure gradient along a micro duct was observed to be

non-constant, and the measured flow rate was much higher than that predicted from the conventional continuum flow model [4].

Nozzle performance at small scales has been studied on a number of occasions. Rothe *et al* reported measurements of temperature and velocity profiles in a nozzle with a 5 mm throat [5]. Grisnik *et al* investigated nozzles with throat diameters on the order of 650 μm [6]. Each of these test cases was machined through conventional macroscale fabrication methods and was orders of magnitude larger than what is now available through MEMS.

Bayt *et al* [7] did a great deal of work on the simulation, fabrication and testing of micro-sized nozzles for generating supersonic flows. Extruded two-dimensional devices, with minimum throat widths averaging 19 μm and 35 μm, were fabricated using micromachining technologies (e.g., deep reactive ion etching (DRIE)) and the anodic wafer bonding technique. However, the etch process resulted in feature enlargement from the photoresist mask which breaks down over time. There was also a variation in etch rate across the wafer due to the asymmetric etchant delivery to the chamber.

**Table 1.** Recommended curing temperature and some properties of SU-8 [8, 9, 15].

Material	Recommended curing temperature (°C)	Glass transition temperature of unpolymerized film (°C)	Coefficient of thermal expansion of polymerized film (ppm/°C)	Young's modulus of polymerized film (GPa)
SU-8	95	50–55	~52	~4

In addition, silicon–glass anodic bonding needs specialized equipment, and is sensitive to the presence of particles and structures on the wafer surface. Therefore, to construct nozzles or other microfluidic devices with a fabrication process that can precisely control the dimensions of microstructures and incorporates a simple and low-cost bonding method is quite attractive and needed. To some extent, SU-8 processing can meet these requirements. SU-8 is a photo definable epoxy developed by IBM and EPFL [8]. It is primarily used as a negative resist that is compatible with standard silicon processing conditions and can be patterned using a standard i-line mask aligner. SU-8 films as thick as 1 mm can be patterned with nearly vertical sidewall profiles. Well-defined, high aspect ratio structures have also been achieved [9, 10]. Furthermore, SU-8 can be partially pre-baked and bonded with a companion wafer by applying pressure and heat. In previous work, an SU-8 bonding layer was used to form sealed microchannels on the order of hundreds of microns [11]. SU-8 bonding is an adhesive bonding in which a polymer film is used as the intermediate bonding material. Compared to anodic bonding, adhesive bonding offers several potential advantages: (1) the bonding temperature can be below 100 °C (depending on the adhesive material); (2) various wafer substrate materials can be joined; (3) the adhesive tolerates, to some extent, particles and structures on the wafer surface as long as their dimensions are lower than the thickness of the adhesive; (4) high bonding strengths can be achieved; (5) it is a low-cost process; (6) many adhesive materials are compatible with standard cleanroom processing. The potential disadvantages of adhesive bonding include limited temperature stability and long-term stability [12].

In this paper, we present an approach for fabricating micronozzles by using low-temperature wafer-level bonding with SU-8. Specifically, we have performed a comprehensive study of the effects of different processing parameters on the status of sealed micronozzles and void formation at the bond interface. A crack-opening method [13] is used to approximately quantify the strength of the bond formed between two SU-8 layers. Instead of drilling holes ultrasonically in the pyrex wafer [7], DRIE is used for creating inlet and outlet ports in the silicon wafer for gas injection and expulsion, which is more compatible with conventional microfabrication techniques. Converging–diverging nozzle structures are formed in SU-8 film using normal lithography, which can precisely control the dimensions of the microstructures [9–11]. These structures are then encapsulated using the SU-8 wafer-level bonding technique, which only requires coarse alignment during bonding and obviates using a commercially available bonder. An interconnection method using capillary needles, O-rings and flexible tubing is employed to interface the micronozzles with a fluid delivery system to measure the upstream and downstream flow rates of gas (N<sub>2</sub>) flowing in the micronozzles.

For the purpose of comparison, micronozzles with the same dimensions are fabricated using DRIE and silicon–glass anodic bonding techniques at the Army Research Lab (ARL). Leakage tests are carried out to verify the feasibility of the SU-8 bonding technique and micro-to-macro interconnection method. The test results show that these developed techniques may extend the flexibility of fabricating and packaging microfluidic devices.

## 2. Experiment

### 2.1. Low-temperature wafer bonding with SU-8

Fabricating encapsulated micronozzles requires a selection of wafer-level bonding tests with SU-8 as the intermediate bonding material. As mentioned above, SU-8 is an epoxy-based negative photoresist. After being exposed to ultraviolet (UV) light and post-exposure bake, SU-8 shows low volume shrinkage and high resistance to most wet chemicals [14]. Table 1 shows the recommended curing temperature and some properties of SU-8 [8, 9, 15]. The general bonding procedure consists of the following steps:

- (1) Clean silicon and pyrex wafers in piranha solutions then dehydrate the wafers at 200 °C for at least 40 min.
- (2) Deposit, pre-bake, expose, post-bake and develop the first SU-8 layer on the silicon wafer.
- (3) Spin-coat and pre-bake the second SU-8 layer on the pyrex wafer.
- (4) Join the two wafers at different bonding temperatures then apply pressure to eliminate trapped air bubbles with a pair of tweezers.
- (5) After the bonded stack cools to room temperature, blanket expose the second SU-8 layer through the pyrex wafer.
- (6) Post-bake the stack with temperature ramping while applying pressure.

### 2.2. Evaluation of the bond quality

We investigated the influence of different parameters on the bond quality. Two methods, direct inspection and crack opening, are used to determine the presence of voids and to evaluate the bond strength. The bond interface is directly inspected through the transparent pyrex glass wafer to identify the status of sealed nozzles and unbonded areas (including macroscopic and microscopic voids). The crack-opening method consists of splitting two bonded wafers with a razor blade and measuring the equilibrium crack length. This technique is based on the equilibrium of elastic forces of the bent separated part of a pair and bonding forces at the crack tip. The surface energy of the bonded wafers is evaluated using the derived equation [13]. Since this method is dependent on the subjective operation of the researcher

**Table 2.** Typical examples and evaluation results of the SU-8 bonding tests.

No	Material	Layer thickness ( $\mu\text{m}$ )	Pre-bake temperature ( $^{\circ}\text{C}$ )	Pre-bake time (min)	Bonding temperature ( $^{\circ}\text{C}$ )	Post-bake temperature ( $^{\circ}\text{C}$ )	Post-bake time (min)	Bond strength ( $\text{J m}^{-2}$ )	Amount of unbonded area (%)	Status of sealed device channels
1	SU-8-50 <sup>a</sup>	50	95	30	75	95	20	–	90	–
2	SU-8-50	50	95	20	75	95	20	0.55	30	Partly blocked
3	SU-8-50	50	95	10	75	95	20	0.56	20	Totally blocked
4	SU-8-50 <sup>b</sup>	50	95	20	75	95	20	0.42	70	Partly blocked
5	SU-8-50	50	95	20	48	95	20	0.51	30	Clear
6	SU-8-5	10	95	12	75	95	10	0.55	20	Partly blocked
7	SU-8-5	10	95	12	48	95	10	0.43	30	Clear
8	SU-8-5	10	95	12	55	95	10	0.44	30	Almost clear

<sup>a</sup> Wafers failed to bond together.

<sup>b</sup> Without applying pressure using tweezers.

and sensitive to measurement errors, it provides only a rough approximation of the bond strength. Due to these limitations, many measurements were taken to improve the evaluation accuracy. Two types of SU-8 with different viscosities ( $265 \text{ mm}^2 \text{ s}^{-1}$  for SU-8-5 and  $14953 \text{ mm}^2 \text{ s}^{-1}$  for SU-8-50) are used to obtain films of different thicknesses. The tests performed using different bonding parameters, the resulting unbonded areas and quantitative evaluations of the bond strength are listed in table 2.

### 2.3. Fabrication process of micronozzles

Micronozzles were fabricated using the above-described SU-8 bonding process. The fabrication process is illustrated in figure 1. The starting material was a silicon wafer (4" diameter; MEMC Electronic Materials, Inc.) with  $2 \mu\text{m}$  thick thermal oxide deposited on both sides. Photoresist layers were spun on both the  $\text{SiO}_2$  layers. The backside (unpolished) resist layer was patterned and developed, and the oxide layer was then etched with buffered HF (30–36% ammonium fluoride, 4–8% hydrofluoric acid and 56–66% distilled water; Transene Company). The combination of resist and oxide was used as the mask for DRIE inlet and outlet ports in the silicon substrate. After DRIE, the resist was stripped, and  $\text{SiO}_2$  membranes were formed on the bottom of the ports. Subsequently, a  $10 \mu\text{m}$  thick SU-8 (Microlithography Chemical Corporation) layer was deposited and patterned on the membranes and other oxide areas to create micronozzle structures. The  $\text{SiO}_2$  membranes were etched away with reactive ion etching (RIE). An SU-8 bonding layer was spun and partially baked on a pyrex wafer (4" diameter; Bullen Ultrasonics). The silicon and pyrex wafers were then brought into contact with SU-8 to SU-8. Blanket exposure through the pyrex wafer and the following post-bake serve to crosslink and solidify the SU-8 bonding layer. The polymerization of SU-8 is examined by observing the resolution and integrity of the microstructures obtained after adopting suitable pre-bake, exposure and post-bake steps based on previous work [8–11, 16]. Thus, wafer-level bonding was realized to produce sealed micronozzles. For comparison, micronozzles of the same

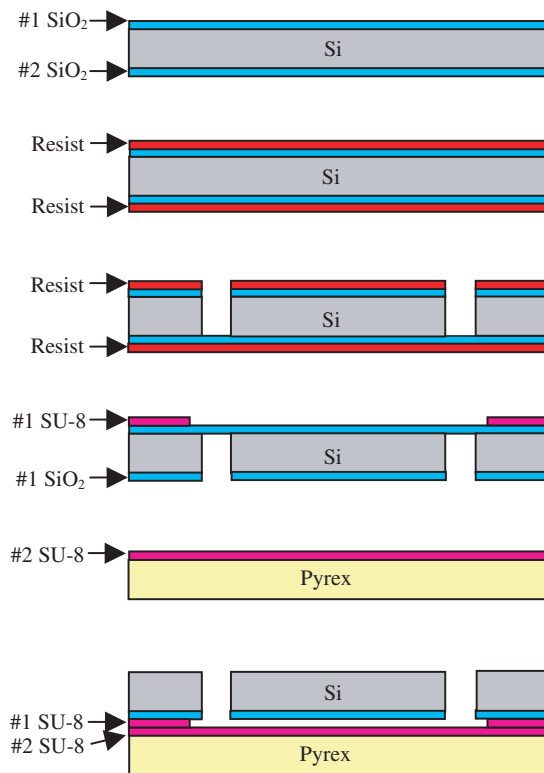


**Figure 1.** Process flow for the fabrication of micronozzles.

dimensions were also fabricated using DRIE and silicon–glass anodic bonding techniques at ARL.

### 2.4. Interconnection and leakage test

Once the device was fabricated, it was packaged to interface with a macroscopic fluid delivery system [17]. As shown in figure 2, this is accomplished by using capillary needles ( $400 \mu\text{m}$  in outer diameter (OD) and  $200 \mu\text{m}$  in inner diameter (ID)) and ethylene propylene O-rings (Apple Rubber). The ID of the O-ring is  $250 \mu\text{m}$ , so a snug fit can be obtained after inserting the needle through the O-ring. The penetration

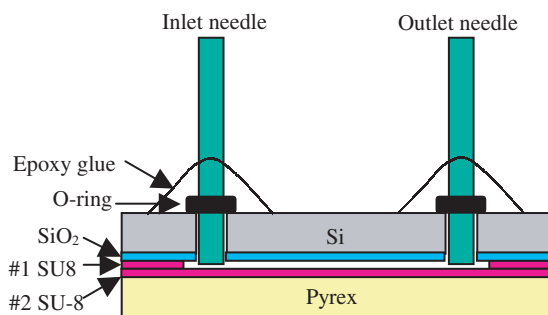


Figure 2. Schematic diagram of interconnection.

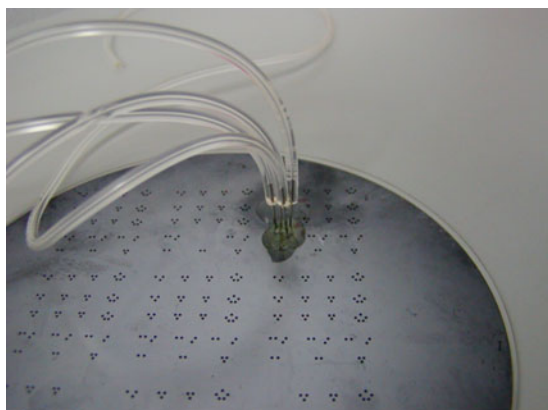
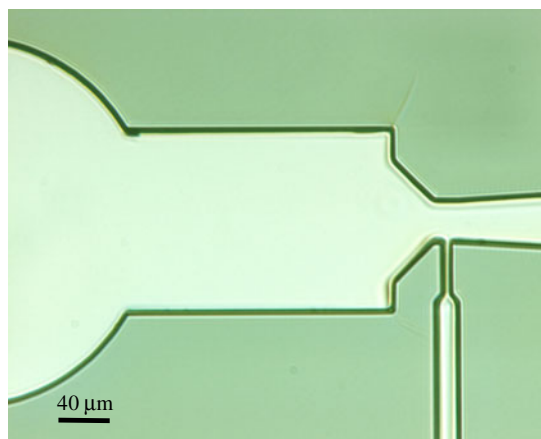
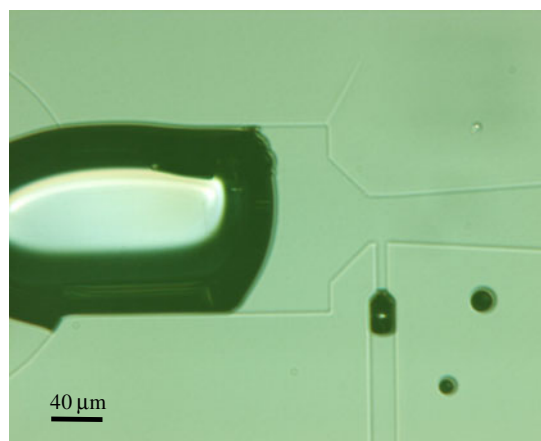


Figure 3. Photograph of a packaged nozzle connected with Tygon tubing.

depth of the assembly was adjusted, by manually controlling the position of the O-ring, such that the capillary needle did not touch the bottom of the micronozzle. The O-ring can also prevent leakage at the contact points. Since the length of the needle (13.45 mm) was much larger than the penetration depth (i.e., the thickness of the silicon wafer, 500  $\mu\text{m}$ ), a probe station was used to hold the needle and to keep it as upright as possible. Following these steps, a droplet of room-temperature curing epoxy glue (Devcon) was applied around the interconnection holes to enhance the holding force. The packaged device was then connected with the gas delivery system through Tygon flexible tubing (2.31 mm in OD and 380  $\mu\text{m}$  in ID, Cole-Parmer Instrument) to conduct leakage tests, as shown in figure 3. Epoxy glue was also applied in the contact area between the needle and Tygon tubing to improve the sealing. In the experiments, working gas ( $\text{N}_2$ ) flowed from a regulated high-pressure cylinder (ranging from 13.8 kPa to 413.7 kPa), through a 0.5  $\mu\text{m}$  filter, past a flow controller, into the nozzle and finally through a flow meter. The filter can prevent contamination from entering the nozzle. Upstream and downstream gas flow rates were read from the flow controller and flow meter (Hastings), respectively. Upstream pressure was measured using a manometer (MKS Instruments) whose tap is connected with the inlet of the nozzle. The exit of the device is vented through the flow meter to atmosphere. Once there is a discrepancy (beyond the measurement accuracy of the flow meter and controller) between the upstream and downstream gas flow rates with increasing pressure, soapy water is applied to the joints of the system (i.e., fittings and interconnections with needles and glue) to locate the leakage



(a)



(b)

Figure 4. Micrographs of sealed nozzle structures using SU-8-50 intermediate layers at two different bonding temperatures: (a) 48  $^{\circ}\text{C}$ ; (b) 75  $^{\circ}\text{C}$ .

by observing the generation of air bubbles. Compared to other leak detection approaches, this method is easier for finding the location of leak and identifying the threshold pressure that the epoxy glue and flexible tubing can stand before leakage happens.

### 3. Results and discussion

#### 3.1. SU-8 bonding process to form sealed micronozzles

Based on previous work [11, 12], two critical parameters, pre-bake time of the SU-8 bonding layer and bonding temperature, were investigated to ensure a good bond while keeping the microchannels free of SU-8 residues. It is observed in the experiments that if the bonding temperature is too low (i.e., room temperature), SU-8 will not be soft enough to make contact with other SU-8 structures, and therefore most areas of the wafers are not bonded. On the other hand, if the bonding temperature is too high ( $>70$   $^{\circ}\text{C}$ , i.e., significantly above the glass transition temperature ( $T_g$ ) of the SU-8 (50–55  $^{\circ}\text{C}$ )), SU-8 will flow into and block the channels because of its relatively high mobility. In our experiments, the optimum bonding temperature is found to be between 45 and 50  $^{\circ}\text{C}$ , slightly lower than the  $T_g$  of SU-8. Figure 4 shows that the

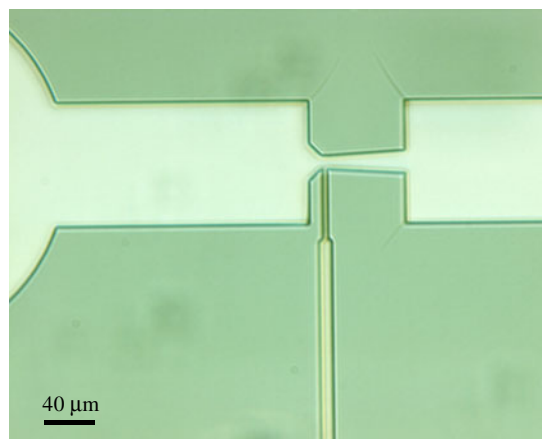
channels are completely free of SU-8 residues at 48 °C while at 75 °C the channels are completely blocked by the seeping of SU-8. Three different pre-bake times, 10, 20 and 30 min, were used for the bond tests. The 20 min bake was found to be suitable for a 50  $\mu\text{m}$  thick SU-8 bonding layer. The 10 min bake caused seepage of SU-8 into the microchannels because of the excessive solvents left in SU-8 while the 30 min bake led to the separation of the two wafers due to the increased hardness of the SU-8 bonding layer. Similar bonding tests were performed with 10  $\mu\text{m}$  thick SU-8 bonding layers. In this case, a 12 min pre-bake was found to be appropriate. Three different bonding temperatures, 48 °C, 55 °C and 75 °C, were explored for the 10  $\mu\text{m}$  thick SU-8 bonding layer. Figure 5 shows that the channels are very clear when bonded at 48 °C. Under 55 °C a small amount of SU-8 was found in the channels while at 75 °C the channels are totally blocked by SU-8. Therefore, it is concluded that SU-8 bonding should be conducted slightly below  $T_g$  to prevent SU-8 from obstructing the microchannels.

Since the bonding step is carried out on a hotplate placed in a commonly used fume hood, air is inevitably trapped between the two bonded wafers, which causes a lot of unbonded portions at the interface. Another consideration is the formation of microscopic gas bubbles with diameters between 10 and 50  $\mu\text{m}$  at the interface due to the evaporation of residual solvents. It is found in our experiments that introducing air escape paths at the bond interface, applying pressure on the bonded pair with tweezers and moving them to push the trapped gases to the escape path are effective to improve the bonding yield. Figure 6 shows a bonded silicon–glass pair with cross-like air escape paths. Most of the device area (around 70%, i.e., the four separated regions) is bonded together. There are, however, some unbonded portions in the device area and near the edge of the bonded pair. Considering that the bonding is achieved without a vacuum environment (i.e., using a commercially available bonder with a vacuum chamber), the yield is acceptable. It is also observed that the bonding process maintains the dimensions and integrity of the converging–diverging nozzle structures.

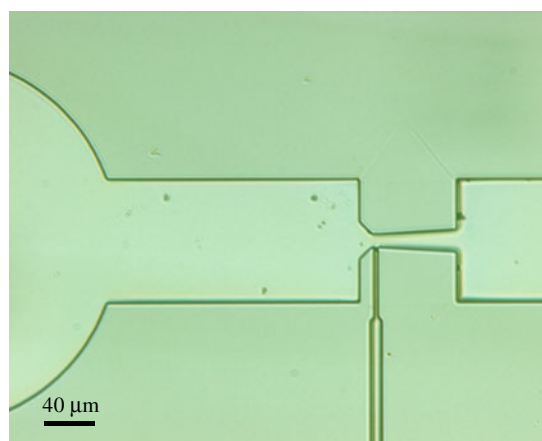
### 3.2. Discussion of bond quality

As mentioned above, the bond quality was evaluated by direct inspection through the transparent pyrex wafer. The amount of unbonded areas for each bond test is listed in table 2. Besides pre-bake time and bonding temperature as discussed above, bonding pressure also has a significant influence on the bond quality, which is indicated by the different unbonded areas between tests 2 and 4 in table 2. Bonding pressure counteracts void formation due to out-gassing substances and trapped air and seals gaps between the bonded wafers that are created by small particles [12].

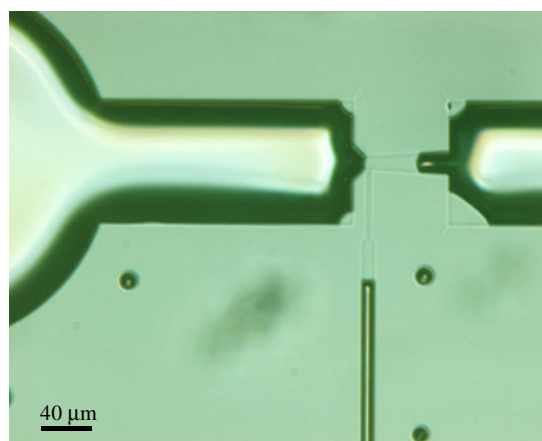
Using the crack-opening method, the surface energy of the bonded wafers was evaluated approximately. For each bonded pair, the razor blade was inserted into three widely spaced portions to minimize the interaction between measurements. Three crack lengths were measured and averaged for each separation area after inserting the blade. The evaluated surface energies for the total of seven bonded pairs are in the range of 0.42–0.56  $\text{J m}^{-2}$ , which are listed in table 2.



(a)



(b)



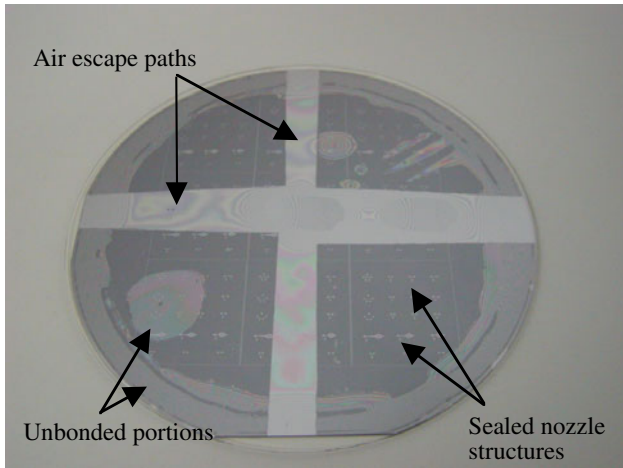
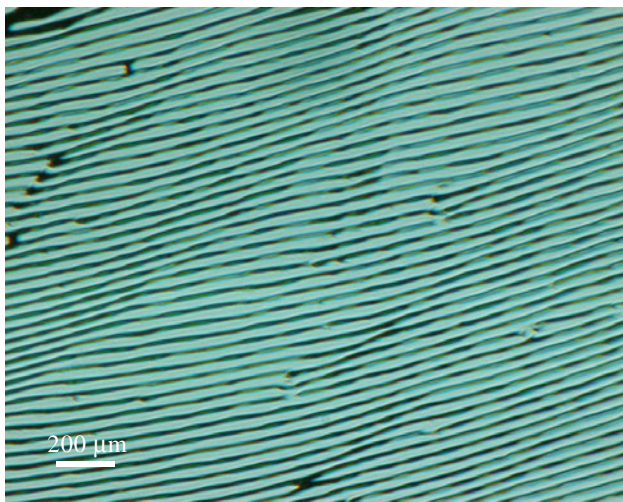
(c)

**Figure 5.** Micrographs of sealed nozzle structures using SU-8-5 intermediate layers at different bonding temperatures: (a) 48 °C; (b) 55 °C and (c) 75 °C.

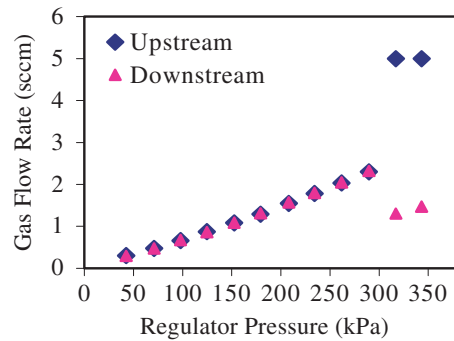
The standard deviation of the measurements is relatively large (i.e., 0.06  $\text{J m}^{-2}$ ), which is due to the irregular shape of the separation area and dependence of the insertion process on the subjective operation. The measured surface energies are comparable to those of some directly bonded PMMA/PMMA (0.44  $\text{J m}^{-2}$ ) and PMMA/Si (0.47  $\text{J m}^{-2}$ ) wafer pairs (samples were annealed in air at 50 °C for 2 h) [18]. The relatively

**Table 3.** Overview of the tested bonding parameters and their impacts on the bond quality. +++ = high influence; ++ = medium influence; + = low influence.

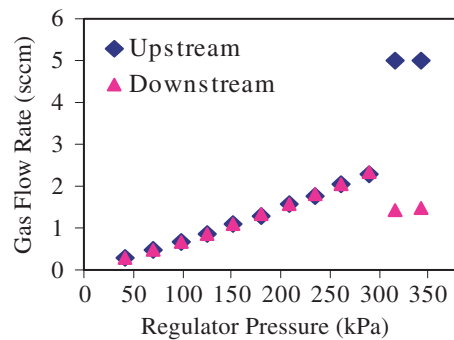
Parameters	Influence on bond quality	Comments/explanation
Bonding temperature	+++	SU-8 bonding just below $T_g$ can prevent the blockage of fluidic channels while keeping good bond.
Bonding pressure	++	Bonding pressure counteracts void formation due to out-gassing substances and trapped air. Bonding pressure also seals gaps between the bonded wafers that are created by small particles and/or structures on the wafer surface.
Pre-bake time	+	Insufficient pre-bake leads to bubble formation due to evaporation of the solvents while excessive pre-bake results in unbonded areas due to the increased hardness of the bonding layer.

**Figure 6.** A pair of silicon-pyrex bonded wafers showing the air escape paths, unbonded portions and sealed nozzle structures.**Figure 7.** A microscope image of one section of the bond interface after splitting two wafers.

strong bond can be attributed to exposing and curing the SU-8 intermediate layer after bonding. These post-bonding steps lead to the molecular rearrangement and interdiffusion, and hence SU-8 chains bridge the initial interface and strengthen the bond. Figure 7 shows fractures through the SU-8 bonding layer after splitting two bonded wafers, which verify the presence of interpenetrating bridges between the SU-8 bonding layer and SU-8 channel layer at the bond interface.



(a)



(b)

**Figure 8.** A comparison between SU-8 bonded and anodically bonded micronozzles for gas flow rates with increasing regulator pressures: (a) SU-8 bonded nozzle; (b) anodically bonded nozzle.

Table 3 gives an overview of the tested bonding parameters and their influences on the bond quality.

### 3.3. Leakage test results

Fabricated micronozzles were packaged and tested using the techniques described in section 2.4. Leakage tests were performed to characterize the seal of the SU-8 bonding and the packaging with the micro-to-macro interconnection method. In the tests, the upstream and downstream flow rates of  $N_2$  gas flowing in a nozzle with a throat width of  $36.4 \mu\text{m}$  were measured by changing the regulator pressure with an increment of  $27.6 \text{ kPa}$ . For comparison, a device of the same dimensions fabricated using DRIE and anodic wafer bonding techniques was also tested. As shown in figures 8(a) and (b), upstream gas flow rates are consistent with downstream ones with increasing regulator pressures up to  $289.5 \text{ kPa}$  for both devices. When the regulator pressure approaches  $317.1 \text{ kPa}$ , leakage begins

to occur in both devices, which is indicated by the discrepancy between the upstream and downstream gas flow rates in figures 8(a) and (b). The leak is observed in the contact area between the needle and Tygon tubing where air bubbles appear after soapy water is applied there. This is due to the deformation of the flexible tubing if the pressure inside the tubing is too high. The testing results demonstrate that the interconnection method using flexible tubing and epoxy glue can be used in a certain pressure range. The seal of SU-8 bonding can also survive this pressure range since the pressure drop in the tubing leading to the nozzle is less than 0.7 kPa at the tested flow rates.

#### 4. Conclusions

A selection of wafer bonding tests was performed using SU-8 as the intermediate bonding material to investigate the influence of different bonding parameters on the bond quality. It was found that bonding temperature, pre-bake time and bonding pressure were critical for realizing good bond while maintaining clear fluidic channels. Sealed micronozzles were fabricated successfully using this fabrication process. The compatibility of this process with traditional fabrication methods enabled the development of hybrid devices that incorporate different materials. The micronozzles were interfaced and tested with the gas flow test setup to verify the feasibility of the fabrication and packaging techniques. The results of the leakage test demonstrate that the low-temperature wafer-level SU-8 bonding process may serve as a complement to conventional microfabrication methods. The characterization results also show that the micro-to-macro interconnection technique is applicable for packaging microfluidic devices working in gaseous environments under standard atmospheric conditions.

#### Acknowledgments

This research was supported by the Northrop Grumman Corporation and the Department of Transportation, Transportation Security Agency Research Center in Atlantic City, NJ. The authors would like to thank the staff of the Army Research Lab (ARL) in Adelphi, MD for fabricating anodically bonded devices, and Nolan Ballew for his help in using the cleanroom facility in the Institute for Research in Electronics and Applied Physics (IREAP) at the University of Maryland in College Park.

#### References

- [1] Dai J, Xu D, Khoo B C and Lam K Y 2000 Navier–Stokes simulations of gas flow in micro devices *J. Micromech. Microeng.* **10** 372–9
- [2] Harley J C, Huang Y, Bau H H and Zemel J N 1995 Gas flow in micro-channels *J. Fluid Mech.* **284** 257–74
- [3] Van den Berg H R, Seldam C A and Gulik P S 1993 Compressible laminar flow in a capillary *J. Fluid Mech.* **246** 1–20
- [4] Gad-el-Hak M 1999 The fluid mechanics of microdevices—the Freeman scholar lecture *J. Fluids Eng.* **121** 5–33
- [5] Rothe D E 1971 Electron-beam studies of viscous flow in supersonic nozzles *AIAA J.* **9** 804–11
- [6] Grisnik S P, Smith T A and Salz L E 1987 Experimental study of low Reynolds number nozzle *AIAA Paper* 87-0092
- [7] Bayt R L, Breuer K S and Ayon A A 1998 DRIE-fabricated nozzles for generating supersonic flows in micropropulsion systems *Proc. Sensors and Actuators Workshop (Hilton Head, USA)* pp 312–5
- [8] Lorenz H, Despont M, Fahrni N, LaBianca N, Renaud P and Vettiger P 1997 SU-8: a low-cost negative resist for MEMS *J. Micromech. Microeng.* **7** 121–4
- [9] Lorenz H, Despont M, Fahrni N, Brugger J, Vettiger P and Renaud P 1998 High-aspect-ratio, ultrathick, negative-tone near-UV photoresist and its applications for MEMS *Sensors Actuators A* **64** 33–9
- [10] Lin C H, Lee G B, Chang B W and Chang G L 2002 A new fabrication process for ultra-thick microfluidic microstructures utilizing SU-8 photoresist *J. Micromech. Microeng.* **12** 590–7
- [11] Jackman R J, Floyd T M, Ghodssi R, Schmidt M A and Jensen K F 2001 Microfluidic systems with on-line UV detection fabricated in photodefinable epoxy *J. Micromech. Microeng.* **11** 263–9
- [12] Niklaus F, Enoksson P, Kalvesten E and Stemme G 2001 Low-temperature full wafer adhesive bonding *J. Micromech. Microeng.* **11** 100–7
- [13] Tong Q-Y and Gösele U 1999 *Semiconductor Wafer Bonding* (New York: Wiley)
- [14] Guérin L J, Bossel M, Demierre M, Calmes S and Renaud Ph 1997 Simple and low cost fabrication of embedded microchannels by using a new thick-film photoplastic *Transducer 97 (Chicago, USA)* pp 1419–21
- [15] LaBianca N C and Gelorme J D 1995 High aspect ratio resist for thick film applications *Proc. SPIE* **2438** 846–52
- [16] Zhang J, Tan K L, Hong G D, Yang L J and Gong H Q 2001 Polymerization optimization of SU-8 photoresist and its applications in microfluidic systems and MEMS *J. Micromech. Microeng.* **11** 20–6
- [17] Li S and Ghodssi R 2002 Development of microfluidic devices for gas centrifuge separation *AVS 49th Int. Symp. (Denver, USA)*
- [18] Spierings G A C M and Haisma J 1994 Direct bonding of organic materials *Appl. Phys. Lett.* **64** 3246–8